Antecedent conditions control thresholds of tile-runoff generation and nitrogen export in intensively managed landscapes

This manuscript has been submitted for publication in Water Resources Research. Please note that this version has not undergone peer review and has not been formally accepted for publication. Subsequent version of this manuscript may have slightly different content. If accepted, the final version of this manuscript will be available via the Peer Reviewed Publication DOI link on the right-hand side of this webpage. Please contact the corresponding author with any questions or concerns.

Molly R. Cain[1], Dong Kook Woo[2], Praveen Kumar[3], Laura Keefer[4], Adam S. Ward[1]

[1]O'Neill School of Public and Environmental Affairs, Indiana University, Bloomington, Indiana, USA
[2]Department of Civil Engineering, Keimyung University, Daegu, Republic of Korea
[3]Department of Civil and Environmental Engineering, University of Illinois at Urbana-Champaign, Urbana, Illinois, USA
[4]Illinois State Water Survey, Champaign, Illinois, USA

Corresponding author:
Molly R. Cain (cainmr@iu.edu)

Key points:

- A tile-runoff threshold emerges as a function of both above- and below-tile antecedent storage.
- Total storm event nitrate load is primarily controlled by the same factors that dictate event tile-runoff.
- Within-event nitrate concentration-discharge relationships reflect a threshold of soil water mobilization.

Abstract

Threshold changes in rainfall-runoff generation commonly represent shifts in runoff mechanisms and hydrologic connectivity controlling water and solute transport and transformation. In watersheds with limited human influence, threshold runoff responses reflect interaction between precipitation event and antecedent soil moisture. Similar analyses are lacking in intensively managed landscapes where installation of subsurface drainage tiles has altered connectivity between the land surface, groundwater, and streams, and where application of fertilizer has created significant stores of subsurface nitrogen. In this study, we identify threshold patterns of tile-runoff generation for a drained agricultural field in Illinois and evaluate how antecedent conditions—including shallow soil moisture, groundwater table depth, and the presence or absence of crops—control tile response. We relate tile-runoff thresholds to patterns of event nitrate load observed across multiple storm events and evaluate how antecedent conditions control within-event nitrate concentration-discharge relationships. Our results demonstrate that an event tile-runoff threshold emerges relative to the sum of gross precipitation and indices of antecedent shallow soil moisture and antecedent below-tile groundwater moisture deficit, indicating that both shallow soil and below-tile storages must be filled to generate significant runoff. In turn, event nitrate load shows a linear dependence on runoff for most time periods, suggesting that subsurface nitrate export and storage can be estimated using runoff threshold relationships and long-term average nitrate concentrations. Finally, within-event nitrate concentration-discharge relationships are controlled by event size and the antecedent tile flow state because these factors dictate the sequence of flow path activation and tile connectivity over a storm event.

Plain language summary:

Improving nutrient management in intensively managed landscapes requires understanding of how human alterations for agriculture have influenced nutrient transport from and storage within the landscape. In addition to creating large subsurface stores of nitrogen through fertilizer application, humans have altered the drainage structure of intensively managed landscapes by installing subsurface drainage (commonly 'tiles') to maintain optimal moisture conditions for crops. Although highly engineered systems, it is unclear how tiles influence the timing and magnitude of water and nutrient export from these landscape. Here, we identify how pre-storm

wetness conditions control rapid, nonlinear changes in tile flow (thresholds). We find that a tile flow initiation threshold results from the sequential filling of first a depleted shallow soil storage and then deeper below-tile groundwater storage. Further, nitrate export reflects tile-runoff thresholds, indicating that the factors controlling tile-runoff are also primary controls on tile nitrate export.

1. Introduction

Nonlinear responses in rainfall-runoff generation (i.e., small changes in catchment wetness leading to large changes in streamflow) have been documented in catchments spanning physiographic and climatic regions (e.g., *Ali et al.*, 2013; *Weiler et al.*, 2005). Nonlinear or threshold changes commonly reflect activation of runoff mechanisms or hydrologic pathways (e.g., *Kirchner*, 2009; *McGuire and McDonnell*, 2010; *Soulsby et al.*, 2015; *Spence*, 2007). Consequently, identifying threshold relationships provides insight into the dominant mechanisms of delivery and sources of water to streams, as well as how the relative importance of mechanisms evolves over timescales ranging from individual events to multiple-year weather patterns. These responses control the transport and fate of water and solutes in the landscape, including the timiFng and magnitude of export (e.g., *Macrae et al.*, 2010; *Stieglitz et al.*, 2003) and the potential for biogeochemical transformation (e.g., *Covino*, 2017; *McMillan et al.*, 2018). While threshold patterns and associated mechanisms have been widely described in forested hillslopes (e.g., *Detty and McGuire*, 2010; *Farrick and Branfireun*, 2014; *James and Roulet*, 2007; *Penna et al.*, 2011), comparable studies are lacking in intensively managed landscapes (IMLs) despite their prevalence. Thus, our overarching objective is to characterize rainfall-runoff threshold relationships and their role in controlling the storage and export of water and solutes in IMLs.

Human intervention has profoundly changed catchment drainage structure and biogeochemical function of IMLs (*Blann et al.*, 2009; *Kumar et al.*, 2018). Throughout humid agricultural regions of the Midwestern U.S., Canada, and northern Europe, subsurface drainage systems (commonly ‘tile drains’ or ‘tiles’) are widely installed to maintain optimal soil moisture conditions for crops. An estimated 56 million acres of U.S. farmland are tile-drained, about 14% of total U.S. cropland (*USDA*, 2017; *Zulauf and Brown,* 2019). Relative to undrained systems, tiles create a physical threshold that alters connectivity between the land surface, groundwater, and streams (*Gedlinske*, 2014; *Kleinman et al.*, 2015; *Macrae et al.*, 2019). Flow through tile drains may represent 40-95% of annual watershed discharge in IMLs (*King et al.*, 2014; *Macrae et al.*, 2007; *Schilling and Helmers*, 2008; *Williams et al.*, 2015). Perhaps unsurprisingly, these dominant flow pathways for water also account for much of the nitrate, phosphorus, and pesticide loading to downstream waterways (e.g., *Baker and Johnson*, 1981; *Buhler et al.*, 1993; *King et al.*, 2015; *Kladivko et al.*, 2001; *Randall and Mulla*, 2001; *Saadat et al.*, 2018; *Sims et al.*, 1998). Moreover, tiles are particularly important during storm events, when a disproportionate amount of annual nutrient loads are mobilized from landscapes to streams (*Royer et al.*, 2006). Despite the widespread installation of tiles and their recognized role in transmitting water and solutes from the landscapes they drain, their role in controlling the timing, magnitude, and sources of runoff and nutrients is not well understood.

Two predominant models exist to describe tile-runoff generation, with contrasting implications for the storage, transformation, and export of water and nutrients from IMLs. One mechanism is based on infiltration in excess of a water holding capacity within the upper soil layers (*Klaus et al.*, 2013), hereafter described as 'top-down' runoff generation. At the beginning of a storm, only a small amount of water reaches the tile via macropores, primarily event water. Once a soil water capacity threshold is reached, soil water contributions are activated and enter preferential flow paths, corresponding to a large increase in tile flow. This conceptual model suggests preferential flow through macropores directly connected to tile drains. It also predicts that tile flow consists primarily of pre-event water and nutrients displaced from the soil matrix of upper soil layers (*Liu et al.*, 2020; *Williams et al.*, 2018). A second, contrasting conceptual model for tile function is based on groundwater table dynamics, hereafter described as 'bottom-up' runoff generation. In this model, the potentiometric surface intersects the tile drain perennially (e.g., *Schilling and Zhang*, 2004), seasonally (e.g., *King et al.*, 2014), or ephemerally (e.g., *Kleinman et al.*, 2015). Consequently, tile flow is initiated in response to groundwater table rise after a storm event. While the two potential tile-runoff generation mechanisms differ, the models agree that a moisture-based threshold is necessary to explain the hydrologic function of tile-drained landscapes. Event response is 'primed' by either pre-event soil moisture or groundwater table elevation. For example, *Lam et al.* (2016) attributed seasonal differences in tile-runoff response to a threshold of soil moisture content in upper soil layers. Other field studies and conceptual models posit groundwater depth is an important factor in tile-runoff generation, where below-tile storage must be filled to raise the groundwater table for bottom-up activation (*Davis et al.*, 2014; *Vidon and Cuadra*, 2010).

In addition to controlling the hydrologic activation of tiles, antecedent conditions also influence the transport of nutrients associated with this runoff. At interannual timescales, IMLs exhibit chemostatic nitrate export regimes, with legacy sources providing a continuous supply of nitrogen (*Basu et al.*, 2010; *Van Meter et al.*, 2016). However at event timescales, stream nitrate concentrations often exhibit systematic variability in response to changing discharge (*Duncan et al.*, 2017). Concentration-discharge (i.e., c-Q) relationships can be interpreted to infer changes in water sources (*Chanat et al.*, 2002; *Evans and Davies*, 1998) and event activation thresholds for runoff mechanisms (*Rose et al.*, 2018). Within-event c-Q commonly takes the form of hysteresis loops, whereby a clockwise rotational pattern occurs when discharge response lags solute response and a counterclockwise rotational pattern occurs when solute response lags discharge response. *Liu et al.* (2020) found that tile drain nitrate c-Q hysteresis patterns tended to be counterclockwise, consistent with predominantly counterclockwise nitrate c-Q observed in streams draining tiled agricultural watersheds (*Blaen et al.*, 2017; *Outram et al.*, 2016; *Williams et al.*, 2018). In contrast, studies in agricultural watersheds which did not report the presence of tiles documented predominantly clockwise nitrate c-Q (*Chen et al.*, 2012; *Jiang et al.*, 2010), suggesting that tiles are a strong influence on transport processes controlling nitrate dynamics within tile-drained catchments.

While hysteretic behavior may show overall tendencies according to landscape type (*Kincaid et al.*, 2020), c-Q dynamics can also vary dramatically between events in response to differences in antecedent conditions and storm characteristics (e.g., *Davis et al.*, 2014). Antecedent wetness conditions and hydroclimatic variables (e.g., precipitation intensity and amount) interact to influence the evolution of hydrologic connectivity in the landscape during a storm, and this connectivity subsequently activates runoff pathways that control c-Q relationships. However, findings of how these factors influence hysteresis patterns in tile-drained catchments vary. For example, *Blaen et al.* (2017) found that an increase in counterclockwise hysteresis was associated with lower soil moisture in the week preceding an event and high rainfall intensity during events. In contrast, *Williams et al.* (2018) found that hysteresis was not significantly correlated with antecedent wetness or storm event size in a majority of watersheds studied, attributing the lack of correlation to consistent groundwater table rise or seasonal differences in nitrate availability.

In this study, we aim to identify how antecedent conditions control thresholds of tile-runoff generation, and, in turn, observed between- and within-event dynamics in nitrate export from the landscape. Building upon existing studies of IMLs that have primarily focused on either top-down or bottom-up tile-runoff generation mechanisms, we test three expectations. First, we expect a tile-runoff threshold to emerge relative to the sum of gross precipitation and an index of antecedent wetness. In other words, a defined volume of storage must be filled to activate significant tile-runoff. This volume will depend upon either (a) antecedent shallow soil moisture, indicating primarily top-down controls, or (b) antecedent below-tile groundwater moisture deficit, indicating primarily bottom-up controls. Next, we expect that patterns of event nitrate load reflect runoff thresholds when evaluated over interannual timescales. Here, we assume a relatively chemostatic nitrate c-Q relationship at the scale of individual 'tilesheds,' such that event load has a linear dependence on event runoff. Finally, we expect antecedent wetness to control within-event nitrate c-Q relationships because threshold processes associated with runoff generation will be manifested in dynamic hydrologic connectivity in the landscape. To test these expectations, we use a combination of empirical data from a tile-drained field in the IML-Critical Zone Observatory and field-scale simulations of coupled water and nitrogen cycles using the *Dhara* model (*Le and Kumar*, 2017; *Woo and Kumar*, 2019).

2. Methods

2.1. Site Description

The study site is the Allerton Trust Farm which is part of the Intensively Managed Landscapes Critical Zone Observatory (IML-CZO) (*Kumar et al.*, 2018; *Wilson et al.*, 2018) located near Monticello, Illinois (40.0250, -88.6606, Figure 1). The region has a humid continental climate, with cold winters (average January temperature of -2°C) and warm summers (average July temperature of 23°C). Monticello receives an annual average precipitation of 1020 mm. Thunderstorms account for 50-60% of annual precipitation (*Angel*, 2003) in Illinois, and about half of thunderstorm days occur in the summer, although storms frequently occur during all seasons.

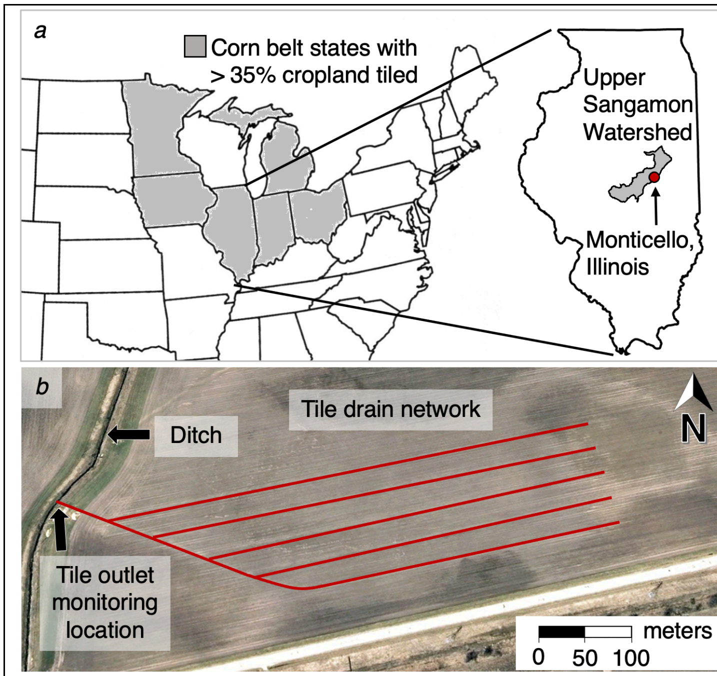

Figure 1. Study site location (a). Gray indicates corn belt states with > 35% cropland tiled (after Zulauf and Brown, 2019). Study site map (b) indicating locations of the subsurface tile drain network (red lines) and location of the tile outlet.

The site is located within the Upper Sangamon River Basin (USRB). The watershed is representative of the glaciated Midwest, characterized by low-gradient topography and poorly draining soils. Soil profiles at the study site reflect glacial deposition patterns, with very deep, poorly draining soils formed under loess, and bedrock depths 50–100 m below the surface. Soils within the monitored tile drainage network belong to the Ipava silt loam and Sable silt clay series (*NRCS*, 2020), and the field is nearly flat with land surface slopes ranging from 0 to 2%. The region has undergone significant anthropogenic changes over the last two decades. Prior to European settlement, the USRB was 90% prairie and 10% forest (*IDNR*, 1999), with forested portions mainly located in riparian zones. Today 90% of land use in the watershed is row crop agriculture, primarily corn and soybeans, and the majority of cropland is tile-drained. Wetlands historically covered about 40-50% of the land area but now make up less than 2% (*IDNR*, 1999; *Rhoads et al.*, 2016), primarily due to the installation of tile drains and ditches which has artificially lowered the water table. Subsurface flows rather than direct surface runoff are the primary pathway by which water and nutrients enter surface waters in the USRB (*Demissie et al.*, 1996), and subsurface flows are mainly conveyed by tile drains (*Botero-Acosta et al.*, 2018).

The farm is about 60 ha total, but the monitored tile network drains an estimated 10 ha based on analysis of aerial photography (*Kratt et al.*, 2020). The drainage network consists of five individual 10-cm diameter perforated pipes, each about 400 m long and spaced 30 m apart, draining into a 10-cm diameter main that empties into a surface drainage ditch. The tiles are about 1–1.2 m below the land surface. The field is not irrigated, so the only water input is precipitation. An annual crop rotation of corn-soybean, a common practice in the Midwestern U.S., is used. During the study period, corn was planted in 2016, 2018, and 2020, and soybean was planted in 2017 and 2019. Prior to the monitoring period, anhydrous ammonia was applied in the fall of 2015 (Table 1). During the monitoring period, 32% urea and ammonium nitrate solution (UAN) was applied in the spring when corn was planted. In spring 2016, 2018, and 2020, 32% UAN was applied as an herbicide carrier in April prior to crop planting. In spring 2018 and 2020, 32% UAN was side-dressed in May after emergence. Each spring, the field was cultivated. During the fall after corn was planted, the field was chisel-plowed to cut and incorporate stalk residue into the soil to preserve soil organic matter and protect against erosion.

Table 1	Nitrogen fertilizer application at field site
Fall 2015	179 kg N ha^{-1}, anhydrous ammonia
Spring 2016	April: 50 kg N ha^{-1}, 32% UAN applied as herbicide carrier
Spring 2018	April: 50 kg N ha^{-1}, 32% UAN applied as herbicide carrier May: 140 kg N ha^{-1}, 32% UAN applied as side-dress
Spring 2020	April: 60 kg N ha^{-1}, 32% UAN applied as herbicide carrier May: 140 kg N ha^{-1}, 32% UAN applied as side-dress

**UAN = urea and ammonium nitrate solution*

2.2. Field and Laboratory Methods

Tile discharge, precipitation, and soil moisture were monitored throughout the 4-year study period at 15 minute intervals (April 2016 to June 2020). Tile discharge was measured within the tile main about 10 m from the outlet using a v-notch weir equipped with Decagon CTD-10 pressure transducers. Precipitation was measured using a Texas Electronics TR-525I tipping bucket rain gauge. Volumetric soil water content (VWC) was measured hourly at 5 cm and 20 cm depths using Decagon 5TE VWC dielectric soil moisture sensors installed in a grassed buffer strip near the tile drain outlet. A Teledyne ISCO 3700 was installed in the tile main near the outlet to automatically collect water samples during periods of tile flow. Samples were collected over a four year period: May–October 2016, February–July 2017, April–June 2019, and January–March 2020. After collection from the ISCO, water samples were filtered using 0.45 µm polypropylene filters and frozen until analysis. Nitrate (NO_3-N) concentrations were determined using ion chromatography.

2.3. Modeling Methods

To supplement field observations with a mechanistic simulation, we used the coupled surface-subsurface flow and soil-vegetation-atmosphere interaction model *Dhara* (*Le and Kumar*, 2017; *Woo and Kumar*, 2019) to simulate the hydrologic and biogeochemical dynamics of a parcel of tile-drained land. The model is used here as a heuristic, providing a basis for interpretation of the processes that are likely to underlie our field observations. The model was previously calibrated and validated for a tile-drained site in DeLand, Illinois that has similar soils, topography, and drainage infrastructure to Allerton Trust Farm and is also located within the USRB. A corn-soybean crop rotation is used at the site, and this rotation is also employed in model simulations. Compared to observed tile flow, simulated flow was muted during high peak flows, which also affected the accuracy of nitrogen loads at high flow. However, tile flow and nitrate loads captured the patterns of the observed data well overall, providing confidence in the use of the simulation results for process investigation. Refer to *Woo and Kumar* (2019) for a detailed description of the parameters and equations governing the model. A schematic diagram of *Dhara* is provided in Supplemental Information (Figure S1). A small number of alterations were made to the model application of *Woo and Kumar* (2019) to address the goals of this study. To simulate the groundwater table, the depth of the model was increased to 3.5 m, with the tile located at 1.2 m below the ground surface. While a horizontal mesh of 1.8 × 1.8 m was maintained, a finer vertical grid resolution of 0.1 m was employed to more accurately simulate the groundwater table and below-tile soil moisture. To account for the additional computational requirements of a finer grid and deeper domain, a smaller representative sub-domain consisting of 55 × 55 grid cells was simulated. Of this domain, the inner 50 × 50 grid cells (90 × 90 m) were analyzed to reduce the effects of numerical boundary conditions. A weather generator was used to create a time series of precipitation as input for the model. Parameters for the weather generator were estimated using meteorological data observed between 1991 and 2010 and obtained from Weather Underground (http://www.wunderground.com). For the simulation, UAN fertilizer was applied at a rate of 15.2 g m^{-2} in the spring prior to planting corn. Model output used in our analysis included hourly time series of soil moisture and tile discharge and daily time series of tile nitrate flux.

2.4. Storm event selection and hydrograph separation

In order to identify relationships between event tile-runoff and antecedent catchment wetness, we first defined a procedure for selecting the tile-runoff volume, gross precipitation, and antecedent moisture conditions associated with discrete storm events. Event selection followed one of two methods, depending on whether precipitation resulted in tile flow, and the same procedures were used for field and model data. If precipitation initiated a tile response, storm event runoff included the period between an initial increase in discharge until either discharge returned to approximately the initial value or increased in response to a different storm. Compound storm events (i.e., those with significant hydrograph overlap between multiple events) were omitted from the runoff threshold analyses. However, compound events were included in the within-event nitrate c-Q analyses, in which we investigated the influence of antecedent tile flow state on event-scale concentration dynamics and flow paths. Events in which snowmelt was expected to contribute to stormflow were also omitted in runoff threshold analyses due to uncertainties in the amount and timing of inputs. While tile flow at the site mainly consisted of stormflow, tiles contributed some baseflow to the drainage ditch during wetter periods. As such, stormflow volumes were determined using the constant slope hydrograph separation method (*Hewlett and Hibbert*, 1967). For storms that resulted in a tile response, gross event precipitation was defined as the total precipitation that occurred up to one day prior to the initial tile storm response until the end of the tile storm response. For storms that did not initiate tile flow, gross event precipitation was calculated as total precipitation that occurred over a day or over consecutive days with precipitation. Gross precipitation over the considered time period had to exceed 1mm to be included in the analysis. Soil moisture values immediately preceding the considered precipitation time period were used to determine an antecedent soil moisture index (ASI), calculated as the total soil water content within the surface soil layer expressed as depth (mm). For this study, we consider the surface soil layer to be 0–0.3 m depth as an indicator of antecedent soil moisture conditions largely independent of groundwater dynamics. ASI is calculated as:

$$ASI = \sum_{i=1}^{n} VWC_i \times D \qquad (1)$$

where VWC_i is the volumetric water content (mm/mm) in the i^{th} sublayer, and D is the layer thickness (mm). We used n = 2 sublayers, with the VWC for 0–5 cm soil depth estimated from the sensor at 5cm depth and VWC for 5-30 cm soil depth estimated from the sensor at 20 cm depth.

2.5. Tile-runoff relationships: calculations and data analysis

We analyzed relationships between storm event tile-runoff and wetness metrics to identify how antecedent wetness controls event tile-runoff. For field data, analyzed wetness metrics included gross precipitation (P_{gross}), ASI, and the sum of gross precipitation and ASI (P_{gross} + ASI). Model analysis included an additional metric of a below-tile groundwater moisture deficit (GW_{def}), calculated as the depth-equivalent unsaturated pore volume below the tile (mm). In other words, GW_{def} represents the depth of water needed to raise the water table to the tile elevation and is calculated as:

$$GW_{def} = -\sum_{i=1}^{n}(VWC_S - VWC_i) * D \tag{2}$$

where VWC_i is the modeled volumetric water content (mm/mm) of the i^{th} layer beneath the tile, VWC_S is the volumetric water content of the soil at saturation (0.56 mm/mm), and D is the layer thickness (100 mm). GW_{def} has a negative value and decreases the overall wetness metric because it indicates a lack of moisture that must be overcome to initiate tile-runoff.

In the absence of field observed below-tile moisture data to explore the effect of bottom-up controls, the antecedent groundwater table position was inferred from tile flow conditions and gross precipitation over the days leading up to the event. Similarly, previous investigations of nonlinear rainfall-runoff response have used proxies for inferring antecedent water storage when soil moisture observations were unavailable, including the duration of inter-storm dry periods (*Graham and McDonnell*, 2010) and the amount of water input required for runoff to initiate (*Ali et al.*, 2015). Here, storm events were categorized as "GW_{def} low," indicating that the groundwater table was expected to be near the tile elevation such that the antecedent below-tile moisture deficit was near zero, if antecedent conditions met either of the following criteria: gross precipitation for the day prior to the event (i.e., 2 days prior to initial tile storm response) exceeded 20 mm or tile flow volume during the 6 days prior to the event exceeded 10 m^3. This procedure was implemented to exclude events in which the antecedent groundwater deficit was high but direct percolation to the tile resulted in a small amount of tile flow. If an event did not meet the above criteria, it was categorized as "GW_{def} high," and the groundwater table was expected to be significantly lower than the tile such that antecedent below-tile moisture deficit was high. We also investigated how the presence or absence of crops affects event tile-runoff by categorizing storm events as occurring either during the growing season or during the non-growing season. Growing season events occurred when crops were present and water uptake was largest, during the months of June, July, August, or September. We expected that large seasonal fluctuations in water uptake and interception of precipitation in IMLs due to presence or absence of crops could pose an additional top-down moisture control on tile-runoff generation. During the growing season, a larger P_{gross} + ASI value would be needed to initiate tile flow due to greater water uptake and interception by crops. Therefore, the runoff initiation threshold relative to P_{gross} + ASI would be larger than during the non-growing season.

To identify potential thresholds within each group and compare threshold relationships between groups (e.g., GW_{def} high versus GW_{def} low), we used linear regression analysis to test for relationships between event tile runoff and wetness metrics for storm events exceeding a wetness value identified within each group. The value above which events were included in above-threshold regression was chosen using a binary logistic regression which modeled the probability of a storm event producing tile flow as a function of the wetness metric being considered. The response variable had two categories, either a storm produced tile flow or not. Storm events were included in the above-threshold linear regression if the they corresponded to a wetness metric at which the modeled probability that the storm would produce tile flow exceeded 0.5. The runoff threshold was estimated as the value at which the linear regression intercepted zero event tile-runoff.

2.6. Nitrate export: calculations and data analysis

Because our expectation that total event nitrate loads reflect runoff thresholds is based on the assumption of a chemostatic nitrate export regime at interannual timescales, we first examined the effect of discharge and time of sampling on nitrate concentrations using analysis of covariance (ANCOVA) and linear regressions. Field nitrate data were categorized into 5 seasonal time periods: Y1 Corn Spring/Summer (May–June 2016), Y1 Corn Summer/Fall (July–Oct 2016), Y2 Soy Spring/Summer (March–June 2017), Y3 Soy Spring/Summer (April–June 2019), and Y4 Winter (Dec 2019–March 2020). We expected that these time periods could reveal differences in nitrate concentration resulting from yearly/seasonal management decisions (e.g., fertilization, crop type). All statistical analyses were conducted in MATLAB, and we use a significance threshold of 0.05. We performed the ANCOVA using the *anovan* function, including discharge as a covariate. This procedure enabled analysis of differences between time periods after the effects of discharge were removed. We followed with a Tukey post hoc test using the *multcompare* function to analyze the main effect of time period. We explored the effect of heteroscedasticity and deviations from normality by performing statistical analyses on $\log_{10}$-transformed data and found no change in results (Table S1). As such, we report results of analyses performed on the non-transformed data. Based on the Tukey post-hoc test, we grouped time periods and performed linear regressions to determine the relationship between discharge and nitrate concentration. Slopes not significantly different from zero would support chemostasis over those time periods. Linear regressions were fit to total event nitrate load and event tile-runoff based on these groupings. We also performed linear regressions on modelled nitrate loads and event tile-runoff for comparison with field data.

Nitrate c-Q relationships were analyzed for field-observed data to evaluate how antecedent conditions influence within-event nitrate dynamics and infer runoff mechanisms. We selected only events in which we obtained nitrate samples throughout the hydrograph (at least 3 samples on the rising limb) and excluded compound events. Thus, 18 distinct storm events were included in the analysis. A similar analysis was not conducted on model data because the daily output of nitrate flux did not typically allow for multiple data points on the rising limb. To quantify event-based hysteretic behavior, we calculated hysteresis (HI) and flushing (FI) indices, which are described in detail in *Vaughan et al.* (2017) and adapted from *Lloyd et al.* (2016) and *Butturini et al.* (2008). Both indices are based on values of either discharge or nitrate concentration normalized over the event to range between 0 to 1:

$$Q_{i,norm} = \frac{Q_i - Q_{min}}{Q_{max} - Q_{min}} \tag{3}$$

$$c_{i,norm} = \frac{c_i - c_{min}}{c_{max} - c_{min}} \tag{4}$$

where Q_i and c_i are the discharge and nitrate concentration values at the ith time step, Q_{min} and c_{min} are the minimum discharge and nitrate concentration values over the storm event, and Q_{max} and c_{max} are the maximum discharge and nitrate concentration values over the storm event. The normalization procedure enables comparison between storm events of different magnitudes. To calculate the hysteresis index, we first linearly interpolated $c_{i,norm}$ to identify concentration values on both the rising and falling limbs at intervals of $Q_{i,norm}$ (i.e., concentrations corresponding to a tile discharge value on both the falling and rising limbs). The hysteresis index was then calculated as:

$$HI = \frac{\sum_{j=1}^{n}(c_{j,rising} - c_{j,falling})}{n} \tag{5}$$

where HI is the hysteresis index, $c_{j,rising}$ and $c_{j,falling}$ are the interpolated values of $c_{i,norm}$ at the jth interval of $Q_{i,norm}$ on the rising and falling limbs respectively, and n is the total number of intervals. For this study, we used n = 10 intervals. Values of HI range from -1 to 1, where positive values indicate clockwise hysteresis (rising limb concentrations greater than falling limb on average) and negative values indicate counterclockwise hysteresis (rising limb concentrations less than falling limb on average). The magnitude of HI represents the strength of hysteresis. The flushing index, indicating the degree of flushing or dilution over the rising limb, was calculated as the difference between the normalized concentration at the time of peak event discharge and the normalized concentration at the beginning of the event. Similarly, FI values range from -1 to 1, with the magnitude representing the degree of flushing or dilution. Positive values indicate an increase in concentration on the rising limb (flushing), and negative values indicate a decrease in concentration on the rising limb (dilution). We consider HI and FI values within 10% of the index range (between -0.1 to 0.1) to be neutral, following *Butturini et al.* (2008) and *Liu et al.* (2020).

3. Results

3.1. Controls of antecedent conditions on tile-runoff: field data

Time series of tile discharge, shallow soil moisture, and precipitation data were used to investigate how antecedent conditions control event tile-runoff. A total of 157 storm events were analyzed, 45 of which resulted in tile-runoff. We found that event runoff depth correlated with gross precipitation ($r^2 = 0.28$, Figure 2b) but not antecedent soil moisture (Figure 2a). When gross precipitation and antecedent soil moisture were summed (P_{gross} + ASI), a threshold relationship emerged, and the above-threshold correlation was larger ($r^2 = 0.39$, Figure 2c) relative to the correlation with gross precipitation alone.

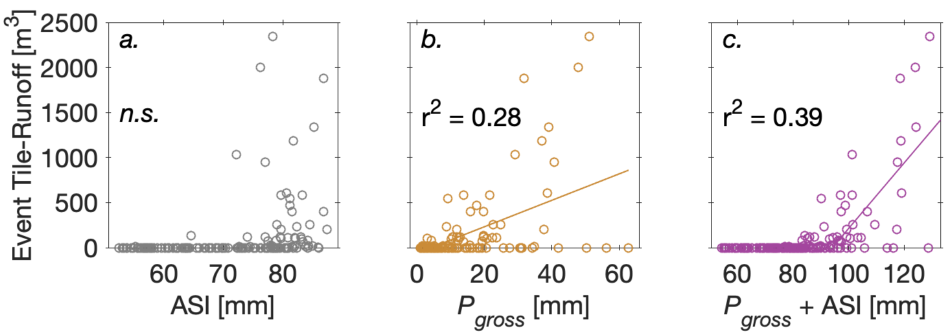

Figure 2. Event tile-runoff for observed storm events and linear regressions relative to (a) antecedent soil moisture index (ASI), (b) gross event precipitation (P_{gross}), and (c) the sum of P_{gross} and ASI (linear fit with intercept of 94 mm). The linear regressions for P_{gross} + ASI is fit to values above a threshold wetness metric. n.s. = not significant

We performed additional analyses to explore whether antecedent below-tile moisture deficit and the presence of crops pose additional controls on tile-runoff response. If below-tile moisture deficit was an important control, we expected that GW_{def} low events would have a strong linear correlation above the P_{gross} + ASI threshold, but GW_{def} high events would be overestimated by the above-threshold trendline for GW_{def} low events. Overall, we found this to be the case: GW_{def} low events showed a strong correlation above the P_{gross} + ASI threshold ($r^2 = 0.79$, Figure 3a), whereas GW_{def} high events showed more spread ($r^2 = 0.13$) and tended to be overestimated by the GW_{def} low trendline. These data indicate that information on available below-tile storage is needed to predict storm event tile-runoff. We also expected that the presence of annual crops would pose an additional control on event tile-runoff. However, both growing season and non-growing season data showed considerable spread around the trend line (Figure 3b, "no crops" r^2

= 0.42 and "crops" r^2 = 0.08). The presence or absence of crops does not contribute additional information to ASI in explaining tile-runoff response.

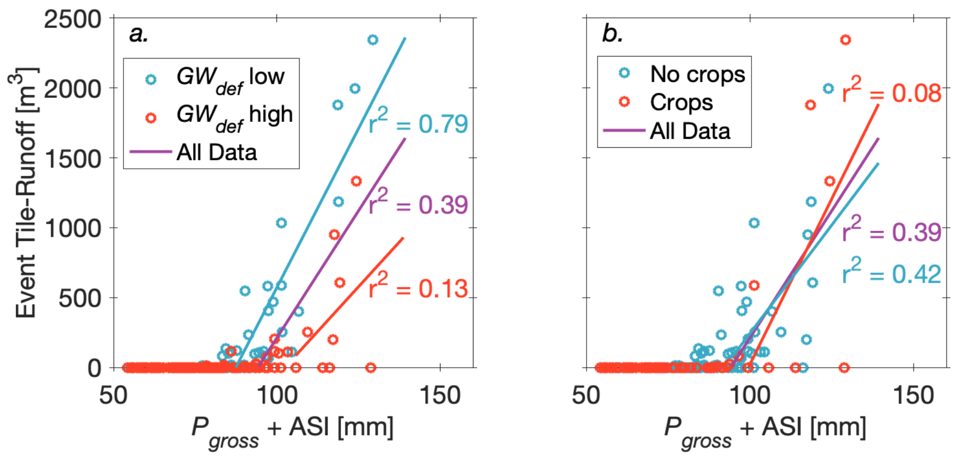

Figure 3. Event tile-runoff for observed events relative to the sum of ASI and gross event precipitation. (a) Events grouped by either "GW_{def} low" or "GW_{def} high" conditions as an indicator of antecedent below-tile groundwater moisture deficit. (b) Events grouped by either "crops" (months of June, July, August, or September) or "no crops" (all other months). Linear regressions are fit to values above a threshold wetness metric. GW_{def} low events have a strong linear correlation above the P_{gross} + ASI threshold, and GW_{def} high events are overestimated by the GW_{def} low trendline. Crop presence or absence does not contribute additional information to ASI in explaining tile-runoff response.

3.2. Controls of antecedent conditions on tile-runoff: model data

In addition to field observations, hydrologic simulations of a tile-drained agricultural site provided 20 years of tile hydrologic response and additional below-tile soil moisture information to investigate how antecedent conditions control tile-runoff. We found that event runoff depth correlated with gross precipitation (r^2 = 0.82) but not ASI or GW_{def} alone (Figure 4a, b, d). A threshold relationship emerged relative to P_{gross} + ASI, with an above-threshold correlation of r^2 = 0.85 (Figure 4c). Similar to field data, the above-threshold correlation for GW_{def} low events improved relative to all data (GW_{def} low r^2 = 0.94 and all data r^2 = 0.85; Figure S2a). On average, the GW_{def} low linear trend overestimated runoff for GW_{def} high events. We expected that adding the numeric below-tile groundwater moisture deficit (GW_{def}) to the catchment wetness metric would result in a clearer threshold trend with event tile-runoff. Indeed, we found that the runoff relationship with P_{gross} + ASI + GW_{def} increased the above-threshold correlation ($r^2 = 0.90$) relative to P_{gross} + ASI. The above-threshold correlation relative to P_{gross} + GW_{def} was similar to P_{gross} + ASI ($r^2 = 0.85$). Thus, considering either GW_{def} or ASI improves our ability to predict event tile-runoff using a threshold relationship. However, the strongest above-threshold trend emerges relative to an antecedent wetness metric which includes both ASI and GW_{def}, indicating that both are strong controls on tile-runoff initiation.

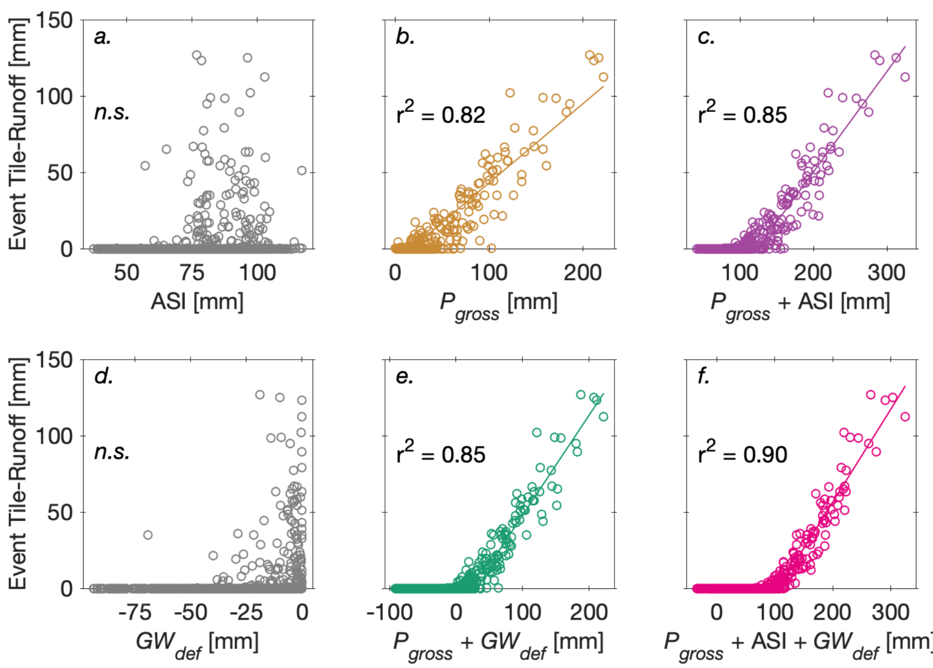

Figure 4. Event tile-runoff for modeled storm events relative to (a) ASI, (b) P_{gross}, and (c) the sum of P_{gross} and ASI (linear fit with intercept of 123 mm), (d) antecedent below-tile groundwater moisture deficit (GW_{def}) (e) the sum of P_{gross} and GW_{def} (linear fit with intercept of 27 mm), and (f) the sum of P_{gross}, ASI, and GW_{def} (linear fit with intercept of 107 mm). Linear regressions for combined wetness indices are fit to values above a threshold wetness metric. n.s. = not significant

3.3. Controls of antecedent conditions on total nitrate load across events

A total of 791 tile water samples were collected over about four years and analyzed for nitrate concentrations (Figure S3). ANCOVA results showed that there is a highly significant interaction between discharge and seasonal time period on nitrate concentration at the 95% confidence interval, $F(4,782) = 6.0$, $p < .001$ (Table S1), indicating that the effect of discharge on nitrate concentration depends on time period. A Tukey-Kramer post hoc test revealed that there is sufficient evidence that the adjusted mean nitrate concentrations are different between most groups ($p < .001$, Table S2) after controlling for discharge. This excludes the difference between

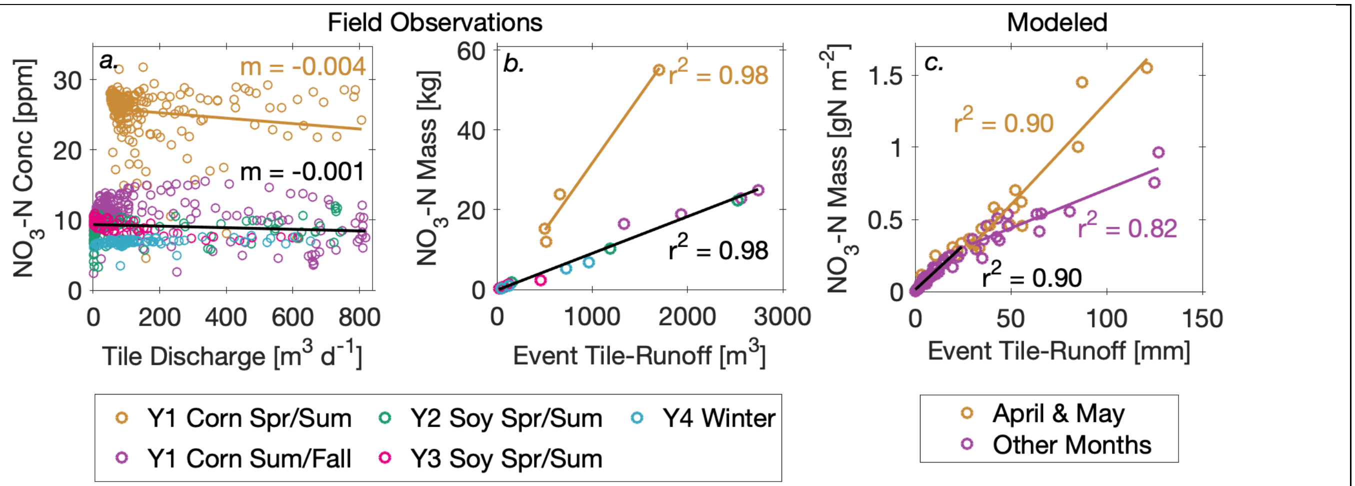

Figure 5. (a) Relationships between observed NO_3-N concentration and tile discharge. Excluding Y1 Corn Spring/Summer which has higher NO_3-N concentrations overall, data exhibit similar concentrations and temporal invariance. (b) Observed event NO_3-N mass load plotted against event tile-runoff shows a strong linear relationship for most time periods, in accordance with the observed chemostatic nitrate export regime. Y1 Corn Spring/Summer is well approximated by a separate linear trendline. (c) Modeled event NO_3-N mass load plotted against event tile-runoff. Events with runoff less than 30 mm are well fit by a single linear trend. Events which exceed this threshold diverge into two trends, with those that occurred in the spring having higher event NO_3-N loads compared to events of the same size that occurred during other times of the year.

Years 2 and 3 Soy Spring/Summer, which is not significant ($p = 0.88$). However, while the magnitude of differences between Y1 Corn Spring/Summer and other time periods were large (14.4–18.4 ppm), differences were small between all other time periods (0.4–4.0 ppm). As such, we fit a linear regression through all data excluding Y1 Corn Spring/Summer, which was fit with a separate regression line (Figure 5a). The first trend line has an intercept of 9.3 ppm and small slope ($m = -0.001$), which is not meaningfully different than zero and indicates a chemostastic response at the interannual timescale. The fit through Y1 Corn Spring/Summer has a higher intercept of 25.8 ppm and more negative slope (m = -0.004), potentially indicating source limitation at higher flows. However, concentrations are also more sporadic over this period. Because nitrate concentrations during time periods other than Y1 Corn Spring/Summer exhibit similar nitrate concentrations and temporal invariance, the relationship between event nitrate load and event tile-runoff for these time periods are well approximated by a linear trend (Figure 5b, $r^2 = 0.98$). While Y1 Corn Spring/Summer is not well approximated by the same trendline as other time periods, nitrate loads during this time period are well approximated by a separate linear trend ($r^2 = 0.98$).

Model data similarly show larger event nitrate loads occurring in the spring compared to other times of the year (Figure 5c). However, whereas field-observed nitrate loads are elevated only during the Y1 Corn Spring/Summer time period, modeled nitrate loads are consistently elevated during the months of April and May regardless of crop type and associated management. Nitrate loads are well approximated by a single linear trend for events with total tile-runoff below about 30 mm. Events which exceed this tile-runoff threshold diverge into two patterns: events which occurred in the spring follow a trend with a larger slope (i.e., have higher nitrate loads for the same event size) compared to events which occurred during other seasons.

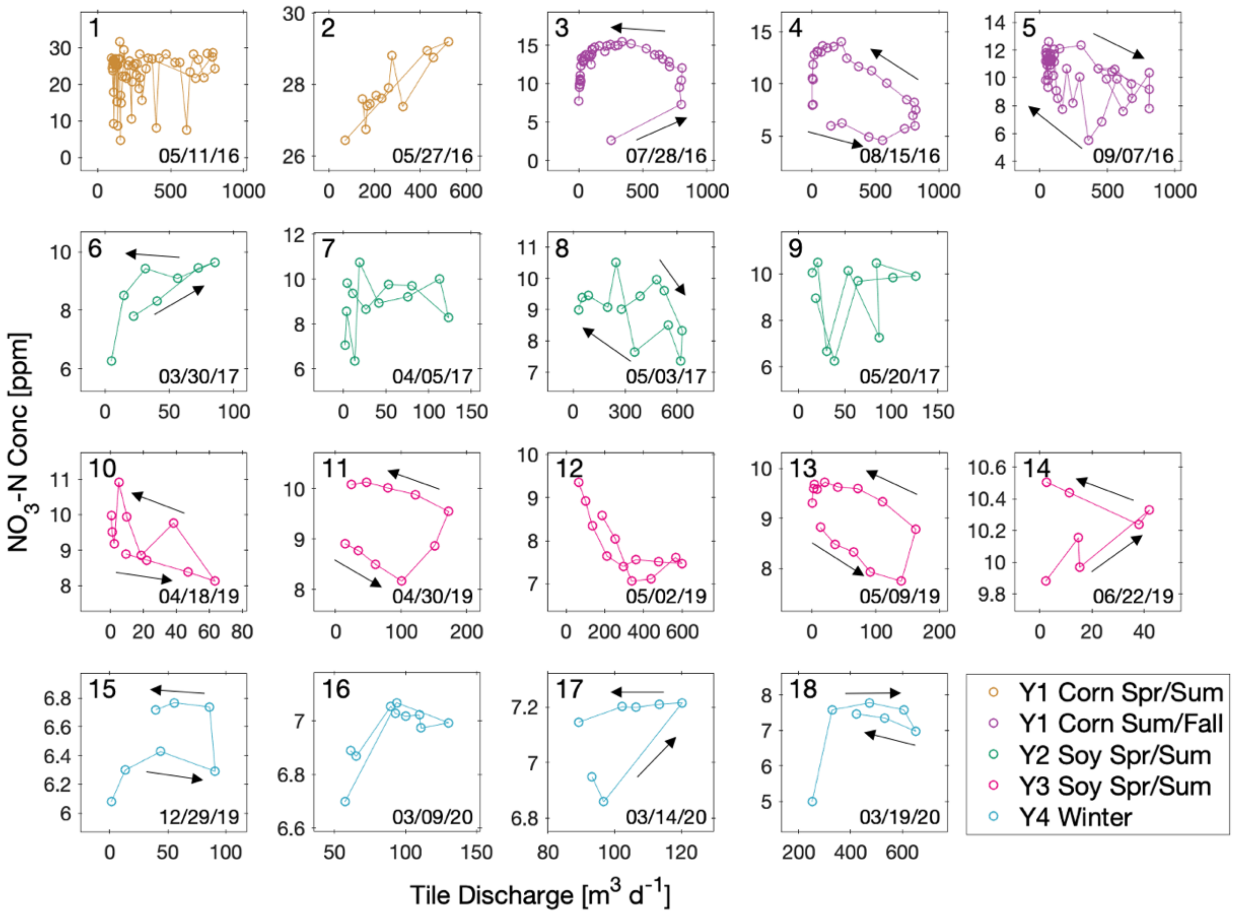

Figure 6. NO_3-N c-Q relationships for observed events. Arrows indicate hysteresis direction for events in which the hysteresis index (HI) magnitude is > 0.1.

507

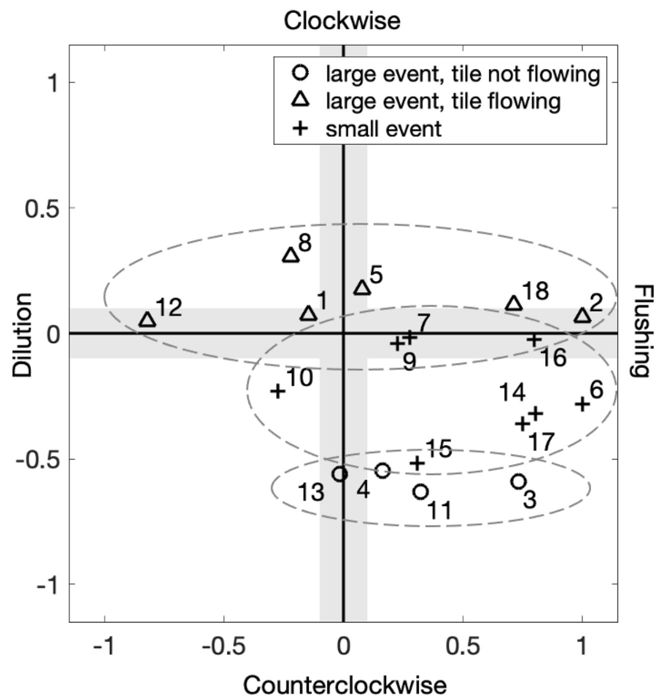

Figure 7. Storm hysteresis (HI, y-axis) and flushing (FI, x-axis) indices for NO_3-N. Numbers correspond to event numbers in Figure 6. Gray shaded regions indicate where indices are neutral (< 0.1). Hysteretic behavior grouped by runoff event size and antecedent tile flow state. Larger events which occurred when there was little to no tile flow at the onset of the event exhibited strong counterclockwise hysteresis. Small events exhibited weak counterclockwise hysteresis to non-hysteretic behavior. Larger events which occurred when the tile was still flowing from a previous event exhibited weak clockwise hysteresis to non-hysteretic behavior.

3.4. Controls of antecedent conditions on nitrate concentration dynamics within events

Of the 18 events analyzed for c-Q relationships, 50% exhibited counterclockwise hysteresis, 17% exhibited clockwise hysteresis, and 33% were non-hysteretic (Figure 6). We did not observe a clear control of ASI or GW_{def} on HI, as would have been exhibited by a trend between HI and ASI or GW_{def}. However, hysteretic behavior grouped by runoff event size and antecedent tile flow state (Figure 7). Larger events (> 150 m^3 d^{-1} peak tile flow) which occurred when there was little to no tile flow at the onset exhibited strong counterclockwise hysteresis (events 3, 4, 11, 23 in Figures 6 and 7). Small events (< 150 m^3 d^{-1} peak tile flow) tended to exhibit weak counterclockwise hysteresis to non-hysteretic behavior (events 6, 7, 9, 10, 14 –17 in Figures 6 and 7). Larger events which occurred when the tile was still flowing from a previous event (i.e., a storm occurred on the falling limb of another event) exhibited weak counterclockwise hysteresis to non-hysteretic behavior (events 1, 2, 5, 8, 12, 18 in Figures 6 and 7).

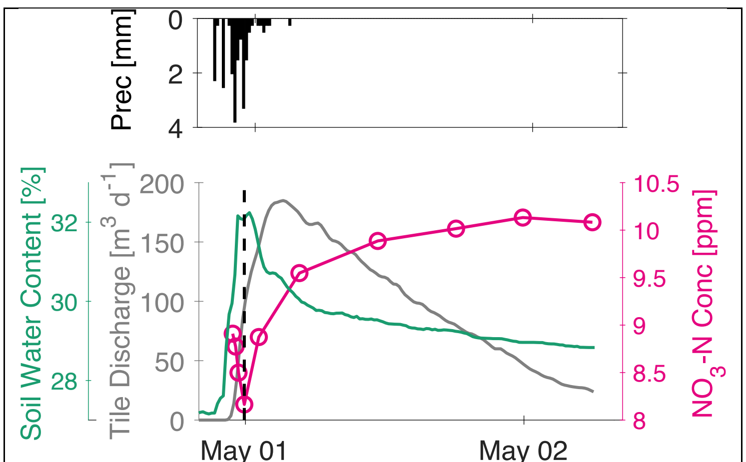

Figure 8. Example tile storm response for event with strong counterclockwise hysteresis. On the rising limb, a decrease in nitrate concentration corresponds with an increase in shallow soil water content until reaching a maximum. The inflection point suggests a threshold of soil water mobilization occurs at a water content of 31–32%.

Storm events had a range of FIs, but the majority of events (67%) had FI > 0.1, indicating nitrate flushing (i.e., an increase in nitrate concentration over the rising limb). Overall, larger events with little to no antecedent tile flow and small events tended to show flushing effects while larger events with high antecedent tile flow showed more variable effects. However, although FI indicates a change in nitrate concentration between the start of an event and the time of peak discharge, the index does not take into account changes in concentration between those times. Visual analysis of nitrate concentration through time reveals inconsistent dilution/flushing over the rising limb. Tile hydrographs had steep rising limbs so water samples were mainly collected on the falling limbs. Of the four events exhibiting strong counterclockwise nitrate c-Q hysteresis, three had high sampling resolution on the rising limb (at least 5 samples). These correspond to an event during Year 1 Corn Summer/Fall (event 4) and two events during Year 3 Soy Spring/Summer (events 11 and 13). These events showed dilution over most of the rising limb prior to a rapid increase in nitrate concentrations before reaching peak discharge (Figures 8 and S4). The decrease in nitrate concentration corresponded with an increase in soil water content until reaching a maximum of about 31–32%, a value near field capacity for silt loam and silt clay soils.

4. Discussion

4.1. Thresholds of tile-runoff generation and nitrogen export

4.1.1. Antecedent catchment wetness controls tile-runoff thresholds

In our empirical and modeling studies, we find evidence for both top-down and bottom-up tile-runoff generation mechanisms. Our analysis of field-observed tile discharge, shallow soil moisture, and precipitation, in conjunction with modeled output including below-tile soil moisture, demonstrates that tile-runoff at the study site is a function of gross precipitation and both below- and above-tile storage controls. Tile-runoff response displays a threshold behavior similar to that observed in forested hillslopes, whereby runoff increases linearly with increasing P_{gross} + ASI after a threshold value is exceeded; prior to the threshold, little runoff is produced in response to rainfall, resulting in an overall relationship reminiscent of a hockey stick shape. However, the above-threshold correlation is not as strong as has been observed in some forested catchments (*Detty and McGuire*, 2010; *Farrick and Branfireun*, 2014). This is potentially due to variation in the observational data set (e.g., number of storm events, available sensor data), intrinsic properties of the system, or the ability of the analysis to capture all relevant storage and runoff generation mechanisms in the tile-drained landscape. We also find that a similar tile-runoff threshold emerges relative to P_{gross} + GW_{def}. Moreover, including both ASI and GW_{def} into the catchment wetness metric further improves the linear runoff relationship, suggesting an additive effect of top-down and bottom-up moisture controls in regulating the tile flow threshold.

Instead of dominance by top-down or bottom-up runoff generation mechanisms, we find that both are important in our study system. In systems where both top-down and bottom-up moisture controls are present, we conceptualize that there is a soil moisture threshold that must be met in the shallow subsurface prior to significant transport to greater depths (Figure 9). Then, if a groundwater deficit is present, below-tile storage must be filled to raise the water table to the elevation of the tile to generate significant runoff. The outcome of this sequential filling of distinct, depleted storages in landscapes parallels that of the fill-and-spill concept initially used to explain threshold runoff behavior at the Panola hillslope (*Tromp-van Meerveld and McDonnell*, 2006a; b). There, depressions in bedrock topography must be filled before water can spill out and become hydrologically connected, generating significant lateral subsurface flow. Whereas the fill and spill mechanism described for the Panola hillslope is a bottom-up runoff generation process with implications for lateral connectivity, at our study site runoff generation is controlled by both top-down and bottom-up moisture, and the relevant storages are oriented vertically. Also in contrast to the steep hillslopes and shallow bedrock systems in many hillslope hydrology studies (e.g., *Tromp-van Meerveld and McDonnell*, 2006a; b), in tile-drained IMLs the water table boundary defines available bottom-up storage and varies temporally. Although the landscape structure and associated runoff generation mechanisms of low-gradient, tile-drained IMLs differs from that of steep, bedrock hillslopes, the conceptual filling and spilling of landscape storages and resultant threshold runoff behavior are similar. Further, fill-and-spill was recently proposed as a framework to more broadly describe runoff generation processes by which landscape storages become progressively filled and connected (*McDonnell et al.*, 2021). Another comparable bottom-up mechanism explaining threshold runoff response in untiled, minimally managed hillslopes is “transmissivity feedback” (*Bishop*, 1991; *Kendall et al.*, 1999). Initially observed in till soils, this describes the process by which rapid lateral flow occurs when the groundwater table rises and encounters surficial soil layers of increasing hydraulic conductivity, often due to the presence of macropore networks. In intensively managed landscapes, the tile elevation threshold controlling lateral subsurface water transmission is analogous to the transmissivity feedback mechanism observed to generate nonlinear runoff response in some forested catchments. Although the water table in tile-drained landscapes is typically constrained too deep to encounter high conductivity shallow soil layers, tiles themselves impart a similar threshold runoff response.

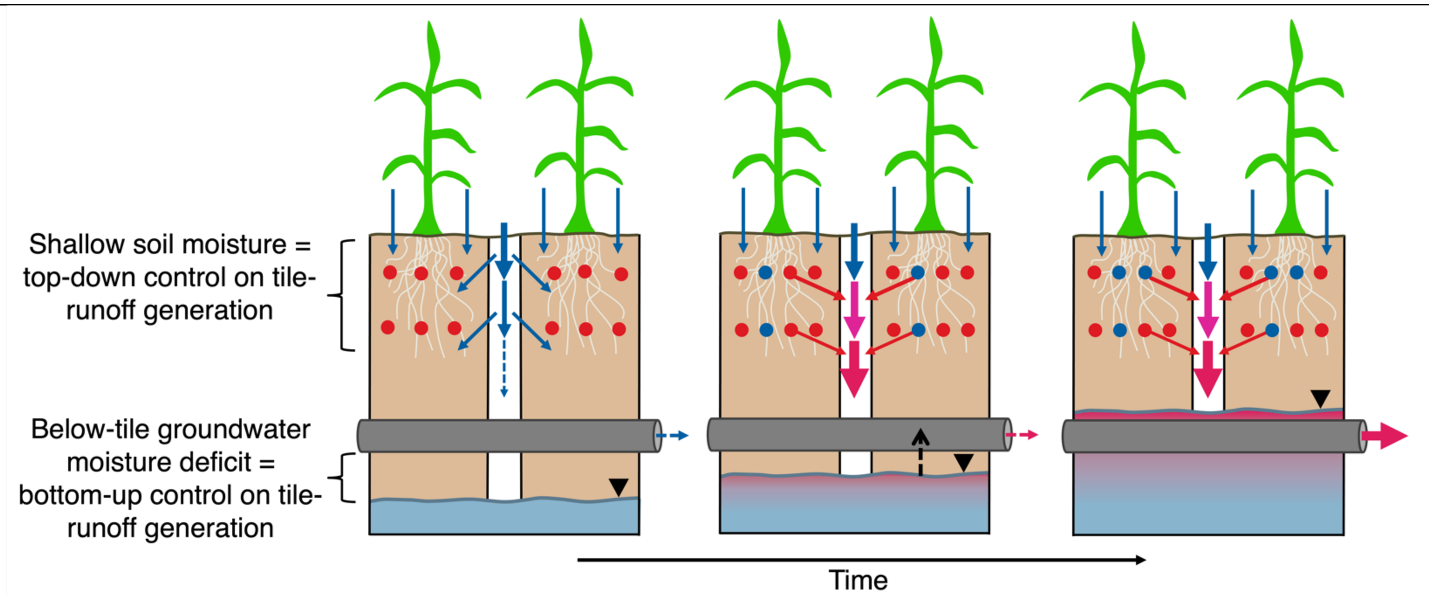

Figure 9. Conceptual tile-runoff generation model for a scenario in which both top-down and bottom-up moisture controls are present. Brown indicates the soil matrix, the white box a preferential flow path, gray a tile drain, and light blue groundwater. Red indicates soil water and dark blue event water. A soil moisture threshold in the shallow subsurface must be met prior to significant transport to greater depths. Initially, water infiltrates the soil matrix and macropores at the beginning of the event, and a small amount of event water reaches the tile drain via preferential flow paths. Once the soil moisture threshold is reached, soil matrix water is mobilized and enters preferential flow paths. If a groundwater deficit is present, below-tile storage must be filled to raise the water table to the elevation of the tile to generate significant runoff. Counterclockwise nitrate c-Q hysteresis, observed during large events with little/no antecedent tile flow, reflects a shift from dilute event water in early runoff to nitrate-laden pre-event water after a soil moisture threshold is exceeded.

In addition to analyzing how antecedent wetness controls tile-runoff response patterns, we examined how distinct landcover regimes in IMLs influence runoff response. In agricultural landscapes dominated by annual crops, vegetation is typically present for periods that coincide with the growing season, resulting in large seasonal fluctuations in evapotranspiration (*Sacks and Kucharik*, 2011; *Shaw*, 1963). Therefore, we expected that vegetation could impart an additional top-down control on subsurface runoff in IMLs via fluctuations in water uptake and interception, with peak water use corresponding to critical crop growth stages (*Al-Kaisi*, 2000). Further, there is evidence that in natural systems ecology and hydrology co-evolve in response to climate, establishing equilibrium conditions between vegetation and water availability to avoid water shortages (*Eagleson*, 1982; *Gao et al.*, 2014; *Troch et al.*, 2015). Due to these linkages between vegetation and root zone soil moisture, soil moisture runoff thresholds may closely reflect vegetation controls in minimally managed systems. In contrast, vegetation patterns in IMLs reflect continuous human manipulation and could act as an independent control on runoff patterns. However, we found no evidence that the presence or absence of crops contributes additional information to ASI in explaining tile-runoff response. This suggests that the influence of crop presence on tile-runoff thresholds is already reflected within the soil moisture metric. Our field data analysis, though, is limited due to the small number of events which produced large runoff during the growing season. In a study of forested headwater catchments at the Coweeta Hydrologic Laboratory, *Scaife and Band* (2017) similarly found little evidence that the P_{gross} + ASI runoff threshold value differed between the dormant and growing season. Nonetheless, their data demonstrate that runoff thresholds vary interannually, largely due to variation in runoff initiation thresholds between growing seasons, and they conclude that interannual runoff thresholds are influenced by ecohydrologic feedbacks with forest evapotranspiration rates.

4.1.2. Antecedent catchment wetness controls nitrate export thresholds

For most time periods, patterns of field-observed event nitrate load reflect tile-runoff thresholds. This relationship arises because tileshed-scale nitrate c-Q is relatively chemostatic when evaluated over multiple events and interannual timescales, leading to a linear dependence of load on runoff. Therefore, the tileshed is primarily transport-limited at the interannual timescale, and nitrate export is controlled by the same factors that dictate event tile-runoff: gross precipitation and antecedent catchment wetness, including both shallow soil moisture and below-tile moisture deficit. An exception to the dominant relationship occurred during Y1 Corn Spring/Summer when nitrate concentrations were higher than other times. This time period, consisting of events in May and June, was distinguished from others in regard to the combination of management and wetness conditions. Events occurred during a rainy period directly following nitrogen fertilizer application. Despite elevated concentrations, nitrate c-Q is still relatively chemostatic during Y1 Corn Spring/Summer such that event nitrate load and runoff show a linear relationship separate from other time periods. Modeled data, in comparison, show that nitrate load is consistently elevated for large events during April and May relative to comparable events during other months, and this occurred regardless of crop and associated management (fertilizer was applied only during corn years). Like field observations, the periods of elevated nitrate export also show a separate, relatively linear relationship with runoff. However, this occurs only above a threshold event runoff of about 30 mm. Below this value, event nitrate load shows a consistent linear dependence on runoff, suggesting that the threshold runoff value corresponds to activation of hydrologic pathways which source variable nitrate loads throughout the year. Within field data, all events from Y1 Corn Spring/Summer exceed a comparable threshold (~300 m^3), preventing further analysis of field data. Taken together, our empirical and model-based results indicate that event nitrate export could be estimated using runoff threshold relationships and long-term average nitrate concentrations (e.g., estimating tile-runoff based on site properties and multiplying this by the average nitrate concentration to calculate load). While this approach would be specific to the threshold relationship at a given site, it is a plausible basis to reconstruct past loading, estimate future responses, or make estimates at unmeasured sites on the basis of similar soil and management characteristics. This could prove useful for predicting nitrate loading from legacy nitrate stores, particularly in the face of increased implementation of conservation practices and precision fertilizer application to reduce nitrogen flushes during large rain events. Still, we note that interactions between management and hydroclimatic variables can overwrite dominant patterns during extreme periods, such as rain shortly after fertilizer application, which is particularly troublesome given that most nitrogen mass is mobilized during a relatively small number of these events (*Royer et al.*, 2006).

In addition to controlling nitrate loading to downstream waterways, tile-runoff thresholds modulate the accumulation of nitrate in groundwater. Tiles reduce recharge of high nitrate concentration soil water to deeper groundwater by providing direct flow paths to streams that bypass deeper groundwater (*Rodvang and Simpkins*, 2001). While the mere presence of tiles is expected to influence spatial variations in groundwater contamination across IMLs (*Power and Schepers*, 1989), emergent runoff thresholds within drained landscapes reveal conditions leading to nitrate storage versus export. For example, a below-threshold event which mobilizes soil water and nitrate but does not raise the groundwater table to intersect the tile would primarily result in storage of nitrate in groundwater. Conversely, an above-threshold event with low antecedent groundwater deficit would result in greater nitrate export. Thus threshold relationships could provide a tool for predicting both the storage and delivery of water and nitrate in IMLs.

4.2. Within-event nitrate c-Q reflects threshold of soil water mobilization

Within-event nitrate c-Q relationships show substantial variation between events, primarily explained by runoff event size and tile flow state at the onset of the event (Figure 7). Hysteretic behavior, in conjunction with these identified controls, provides insight into tile water source activation and transport mechanisms during storm events. The most common nitrate c-Q relationship we observed was counterclockwise hysteresis (50% of events), consistent with studies examining nitrate c-Q in tile flow (*Liu et al.*, 2020) and streams draining tiled watersheds (*Blaen et al.*, 2017; *Outram et al.*, 2016; *Williams et al.*, 2018). This dominant pattern is attributed to a shift from primarily event water in early runoff (typically dilute in nitrate) to nitrate-laden pre-event water sourced from the soil matrix on the falling limb (*Kennedy et al.*, 2012; *Liu et al.*, 2020; *Williams et al.*, 2018; *Woo and Kumar*, 2019). *Klaus et al.'s* [2013] two-phase conceptual flow model, based on a series of tracer experiments, further suggests that the water source transition results from a moisture-based mobilization threshold within upper soil layers. Early in a storm, a small amount of tile flow is generated via macropores, mainly consisting of event water. After a threshold near-saturation moisture is reached within upper soil layers, soil water contributions activate and enter vertical preferential flow paths, and tile flow consists of mainly soil water. While soil water that reaches the saturated zone likely mixes with a small amount of older groundwater, we expect the shallow saturated zone is stratified (*Fenelon and Moore*, 1998; *Jiang and Somers*, 2009) such that tile flow resembles recent soil water.

In our data, the transition from event to soil water is reflected by strong counterclockwise hysteresis during large events which occurred when there was little to no tile flow at the event onset (Figure 9). We expect that during small events, the threshold of soil water mobilization was not reached so c-Q shows weak to no counterclockwise hysteresis (Figure S5). Likewise, large events that occur when the tile is already flowing (i.e., when the tile is initially connected to the water table) do not reflect the transition from event to soil-derived water because tile water is already composed of primarily pre-event water at the beginning of an event. Thus, tile flow exhibits non-hysteretic behavior or weak clockwise hysteresis. Although the tight coupling between tile flow and nutrient load observed in this study indicates that nitrate dynamics were primarily transport-limited, the latter behavior may indicate nitrate source exhaustion when consecutive storm events occurred. Further, while small events observed in this study tended to occur when there was little to no tile flow, we expect that small events which occur when the tile is flowing prior to the event would similarly exhibit weak to no hysteresis, following the same rationale described above.

In addition to hysteretic behavior, we also analyzed nitrate flushing or dilution over the rising limb. Although the majority of events had an overall flushing effect (FI > 0.1), rising limbs often exhibited periods of both dilution and flushing. This is evident in the three events with strong counterclockwise hysteresis (i.e., those capturing the transition from event to pre-event water) in which high sampling resolution was achieved over the rising limb (events 4, 11, and 13; Figures 8 and S4). An initial period of nitrate dilution is followed by a period of flushing. The decrease in nitrate concentration corresponds with an increase in soil moisture prior to both reaching an inflection point. This relationship suggests that the source of tile drain water shifted once a water storage threshold was exceeded, further supporting interpretation of counterclockwise hysteresis as the result of a soil moisture mobilization threshold. For all events, the inflection point occurred when shallow soil water content exceeded 31–32% soil water content. We expect that this soil water content represents the threshold of soil water mobilization within soils at the site. The initial decrease in nitrate concentrations may result from event water depleting nitrate stored within preferential flow paths or on the soil surface. Another potential explanation for the initial decrease in concentration is that water was transported faster than nitrate could be dissolved or mobilized. After the soil moisture threshold is reached, soil matrix water and associated nitrate mobilize, resulting in a rapid increase in nitrate. The threshold of soil water mobilization occurred prior to peak tile discharge, 1–2 hours after the initial increase in tile discharge.

5. Conclusions

In this study, we investigated how antecedent conditions control thresholds of tile-runoff generation and nitrate loads between events, as well as nitrate c-Q relationships within events. First, we expected a tile-runoff threshold would emerge relative to the sum of gross precipitation and an antecedent catchment wetness index reflecting either shallow soil moisture, indicating top-down runoff generation, or below-tile groundwater moisture deficit, indicating bottom-up runoff generation. Instead, we found that the most distinct runoff threshold and linear response emerged as a combination of both top-down and bottom-up controls, quantified as the sum of gross precipitation, antecedent soil moisture index (ASI), and below-tile groundwater moisture deficit (GW_{def}). Moreover, our results demonstrate a simple additive effect of below- and above-tile storage in determining the threshold of tile-runoff initiation.

Next, we expected that event nitrate load would reflect runoff threshold relationships. We found this to be the case for most of the study period, with the exception of a two-month period when wet conditions directly followed fertilizer application and led to elevated nitrate export. Therefore, although interactions between management and hydroclimatic variables can overwrite dominant patterns, under most conditions export of accumulated nitrate is controlled by the same factors controlling tile-runoff and can be accurately predicted using runoff threshold relationships. Finally, we expected that antecedent wetness conditions would control within-event nitrate c-Q relationships. While we did not observe a clear control of ASI or GW_{def} on HI, we found that hysteretic behavior grouped by antecedent tile flow state and runoff event size. Our results suggest that these factors are the dominant controls on event-scale nitrate c-Q because they determine the sequence of flow path activation and tile connectivity over a storm event. Further, the relationship between nitrate concentration and soil water content timeseries indicate a threshold of soil water mobilization, a key mechanism underpinning event-scale nitrate dynamics.

Understanding the hydrologic functioning of tile-drained IMLs is critical to developing accurate predictions of downstream water quality, particularly in the context of a changing climate and continued intensive agriculture to meet growing demands. This study contributes to this area of research by developing a simple model for tile-runoff generation based on the additive effects of top-down and bottom-up moisture controls. Our results suggest that tile-runoff threshold relationships are a promising framework for predicting the storage and delivery of water and nitrate in IMLs under varying antecedent conditions. Catchment classification based on threshold runoff response characteristics has been proposed as a basis for developing a unified hydrologic theory to advance predictive understanding of runoff response as a function of physical controls and climate (*Ali et al.*, 2013). Intensively managed agricultural landscapes comprise a distinct physiographic category, commonly characterized by subsurface drainage, low-gradient topography, anthropogenic nutrient inputs, and transpiration regimes modulated by the seasonal presence or absence of crops. While site-specific variations in tile depth and spacing, soil, climate, and management will influence the slope and intercept of the threshold relationship, this framework can be applied across tile-drained landscapes to support watershed management. Parallel to the approach of using representative hydrologic response units to scale mechanistic understanding at one scale to integrated basin-scale responses (*Buttle*, 2006), the concept of 'representative unit tilesheds' could be used to aggregate individual contributions to larger-scale predictions.

Acknowledgements: Financial support was provided by the U.S. National Science Foundation (NSF) Grants EAR 1331906 for the Critical Zone Observatory for Intensively Managed Landscapes (IML-CZO) and EAR 2012850 for the CINet: Critical Interface Network in Intensively Managed Landscapes. The Illinois State Water Survey provided critical logistical support. We extend our thanks to Hayden Wennerdahl and Donald Keefer for assistance in the field and Ben Wilkins, Greg Michalski, and Lisa Welp for sample processing. Our thanks also to two anonymous reviewers who provided comments that improved the quality of this manuscript. We would like to acknowledge that the study site is located on the traditional lands of the Kickapoo people. The authors report no conflicts of interest. The data used in this publication are accessible via HydroShare (http://www.hydroshare.org/resource/fa4c995da5924331906bc4607f5cc77b).

References

Al-Kaisi, M. (2000), Crop water use or evapotranspiration, *Integrated Crop Management News, 2053.*

Ali, G., C. J. Oswald, C. Spence, E. L. Cammeraat, K. J. McGuire, T. Meixner, and S. M. Reaney (2013), Towards a unified threshold-based hydrological theory: necessary components and recurring challenges, *Hydrol. Process.*, *27*(2), 313-318.

Ali, G., D. Tetzlaff, J. J. McDonnell, C. Soulsby, S. Carey, H. Laudon, K. McGuire, J. Buttle, J. Seibert, and J. Shanley (2015), Comparison of threshold hydrologic response across northern catchments, *Hydrol. Process.*, *29*(16), 3575-3591.

Angel, J. (2003), Climate of Illinois Narrative, Illinois State Water Survey, State Climatologist Office: https://www.isws.illinois.edu/statecli/General/Illinois-climate-narrative.htm. Date accessed: June 2020.

Baker, J., and H. Johnson (1981), Nitrate-Nitrogen in Tile Drainage as Affected by Fertilization 1, *Journal of Environmental Quality*, *10*(4), 519-522.

Basu, N. B., et al. (2010), Nutrient loads exported from managed catchments reveal emergent biogeochemical stationarity, *Geophys. Res. Lett.*, *37*(23), n/a-n/a.

Bishop, K. (1991), Episodic increases in stream acidity, catchment flow pathways and hydrograph separation, *Ph. D. thesis, Univ. of Cambridge*.

Blaen, P. J., K. Khamis, C. Lloyd, S. Comer-Warner, F. Ciocca, R. M. Thomas, A. R. MacKenzie, and S. Krause (2017), High-frequency monitoring of catchment nutrient exports reveals highly variable storm event responses and dynamic source zone activation, *Journal of Geophysical Research: Biogeosciences*, *122*(9), 2265-2281.

Blann, K. L., J. L. Anderson, G. R. Sands, and B. Vondracek (2009), Effects of Agricultural Drainage on Aquatic Ecosystems: A Review, *Crit. Rev. Environ. Sci. Technol.*, *39*(11), 909-1001.

Botero-Acosta, A., M. L. Chu, and A. J. Stumpf (2018), Impacts of environmental stressors on the water resources of intensively managed hydrologic systems, *Hydrol. Process.*, *32*(19), 2947-2962.

Buhler, D., G. Randall, W. Koskinen, and D. Wyse (1993), Atrazine and alachlor losses from subsurface tile drainage of a clay loam soil, *Journal of environmental quality*, *22*(3), 583-588.

Buttle, J. (2006), Mapping first-order controls on streamflow from drainage basins: the T3 template, *Hydrological Processes: An International Journal*, *20*(15), 3415-3422.

Butturini, A., M. Alvarez, S. Bernal, E. Vazquez, and F. Sabater (2008), Diversity and temporal sequences of forms of DOC and NO3-discharge responses in an intermittent stream: Predictable or random succession?, *Journal of Geophysical Research: Biogeosciences*, *113*(G3).

Chanat, J. G., K. C. Rice, and G. M. Hornberger (2002), Consistency of patterns in concentration-discharge plots, *Water Resources Research*, *38*(8), 22-21-22-10.

Chen, N., J. Wu, and H. Hong (2012), Effect of storm events on riverine nitrogen dynamics in a subtropical watershed, southeastern China, *Science of the Total Environment*, *431*, 357-365.

Covino, T. (2017), Hydrologic connectivity as a framework for understanding biogeochemical flux through watersheds and along fluvial networks, *Geomorphology*, *277*, 133-144.

Davis, C. A., A. S. Ward, A. J. Burgin, T. D. Loecke, D. A. Riveros-Iregui, D. J. Schnoebelen, C. L. Just, S. A. Thomas, L. J. Weber, and M. A. St. Clair (2014), Antecedent moisture controls on stream nitrate flux in an agricultural watershed, *Journal of environmental quality*, *43*(4), 1494-1503.

Demissie, M., L. Keefer, D. Borah, V. Knapp, S. Shaw, K. Nichols, and D. Mayer (1996), Watershed monitoring and land use evaluation for the Lake Decatur watershed, Illinois State Water Survey.

Detty, J., and K. McGuire (2010), Threshold changes in storm runoff generation at a till-mantled headwater catchment, *Water Resources Research*, *46*(7).

Drewry, D. T., P. Kumar, S. Long, C. Bernacchi, X.-Z. Liang, and M. Sivapalan (2010a), Ecohydrological responses of dense canopies to environmental variability: 1. Interplay between vertical structure and photosynthetic pathway, *Journal of Geophysical Research: Biogeosciences*, *115*(G4).

Drewry, D. T., P. Kumar, S. Long, C. Bernacchi, X.-Z. Liang, and M. Sivapalan (2010b), Ecohydrological responses of dense canopies to environmental variability: 2. Role of acclimation under elevated CO2, *Journal of Geophysical Research: Biogeosciences*, *115*(G4).

Duncan, J. M., C. Welty, J. T. Kemper, P. M. Groffman, and L. E. Band (2017), Dynamics of nitrate concentration-discharge patterns in an urban watershed, *Water Resources Research*, *53*(8), 7349-7365.

Eagleson, P. S. (1982), Ecological optimality in water-limited natural soil-vegetation systems: 1. Theory and hypothesis, *Water Resources Research*, *18*(2), 325-340.

Evans, C., and T. D. Davies (1998), Causes of concentration/discharge hysteresis and its potential as a tool for analysis of episode hydrochemistry, *Water Resources Research*, *34*(1), 129-137.

Farrick, K. K., and B. A. Branfireun (2014), Soil water storage, rainfall and runoff relationships in a tropical dry forest catchment, *Water Resources Research*, *50*(12), 9236-9250.

Fenelon, J. M., and R. C. Moore (1998), Transport of Agrichemicals to Ground and Surface Water in a Small Central Indiana Watershed, *Journal of Environmental Quality*, *27*(4), 884-894.

Gao, H., M. Hrachowitz, S. J. Schymanski, F. Fenicia, N. Sriwongsitanon, and H. Savenije (2014), Climate controls how ecosystems size the root zone storage capacity at catchment scale, *Geophys. Res. Lett.*, *41*(22), 7916-7923.

Gedlinske, B. B. (2014), Agricultural Drainage Tiles: An Overview of their Use, Benefits, and effect on Hydrology and Water Quality.

Graham, C. B., and J. J. McDonnell (2010), Hillslope threshold response to rainfall: (2) Development and use of a macroscale model, *J. Hydrol.*, *393*(1), 77-93.

Hewlett, J. D., and A. R. Hibbert (1967), Factors affecting the response of small watersheds to precipitation in humid areas, *Forest hydrology*, *1*, 275-290.

IDNR (1999), *Upper Sangamon River Area Assessment: Living resources*, Illinois Department of Natural Resources.

James, A. L., and N. T. Roulet (2007), Investigating hydrologic connectivity and its association with threshold change in runoff response in a temperate forested watershed, *Hydrological Processes: An International Journal*, *21*(25), 3391-3408.

Jiang, R., K. P. Woli, K. Kuramochi, A. Hayakawa, M. Shimizu, and R. Hatano (2010), Hydrological process controls on nitrogen export during storm events in an agricultural watershed, *Soil Science & Plant Nutrition*, *56*(1), 72-85.

Jiang, Y., and G. Somers (2009), Modeling effects of nitrate from non-point sources on groundwater quality in an agricultural watershed in Prince Edward Island, Canada, *Hydrogeology Journal*, *17*(3), 707-724

Kendall, K. A., J. Shanley, and J. J. McDonnell (1999), A hydrometric and geochemical approach to test the transmissivity feedback hypothesis during snowmelt, *J. Hydrol.*, *219*(3-4), 188-205.

Kennedy, C. D., C. Bataille, Z. Liu, S. Ale, J. VanDeVelde, C. R. Roswell, L. C. Bowling, and G. J. Bowen (2012), Dynamics of nitrate and chloride during storm events in agricultural catchments with different subsurface drainage intensity (Indiana, USA), *J. Hydrol.*, *466*, 1-10.

Kincaid, D. W., E. C. Seybold, E. C. Adair, W. B. Bowden, J. N. Perdrial, M. C. H. Vaughan, and A. W. Schroth (2020), Land Use and Season Influence Event-Scale Nitrate and Soluble Reactive Phosphorus Exports and Export Stoichiometry from Headwater Catchments, *Water Resources Research*, *56*(10), e2020WR027361.

King, K., N. Fausey, and M. Williams (2014), Effect of subsurface drainage on streamflow in an agricultural headwater watershed, *J. Hydrol.*, *519*, 438-445.

King, K. W., M. R. Williams, M. L. Macrae, N. R. Fausey, J. Frankenberger, D. R. Smith, P. J. A. Kleinman, and L. C. Brown (2015), Phosphorus Transport in Agricultural Subsurface Drainage: A Review, *Journal of Environmental Quality*, *44*(2), 467-485.

Kirchner, J. W. (2009), Catchments as simple dynamical systems: Catchment characterization, rainfall-runoff modeling, and doing hydrology backward, *Water Resources Research*, *45*(2).

Kladivko, E. J., L. C. Brown, and J. L. Baker (2001), Pesticide transport to subsurface tile drains in humid regions of North America, *Crit. Rev. Environ. Sci. Technol.*, *31*(1), 1-62.

Klaus, J., E. Zehe, M. Elsner, C. Külls, and J. McDonnell (2013), Macropore flow of old water revisited: experimental insights from a tile-drained hillslope, *Hydrol. Earth Syst. Sci.*, *17*(1), 103-118.

Kleinman, P. J. A., D. R. Smith, C. H. Bolster, and Z. M. Easton (2015), Phosphorus Fate, Management, and Modeling in Artificially Drained Systems, *Journal of Environmental Quality*, *44*(2), 460-466.

Kratt, C. B., D. K. Woo, K. N. Johnson, M. Haagsma, P. Kumar, J. Selker, and S. Tyler (2020), Field trials to detect drainage pipe networks using thermal and RGB data from unmanned aircraft, *Agricultural Water Management*, *229*, 105895.

Kumar, P., P. V. Le, A. T. Papanicolaou, B. L. Rhoads, A. M. Anders, A. Stumpf, C. G. Wilson, E. A. Bettis III, N. Blair, and A. S. Ward (2018), Critical transition in critical zone of intensively managed landscapes, *Anthropocene*, *22*, 10-19.

Lam, W. V., M. L. Macrae, M. C. English, I. P. O'Halloran, J. M. Plach, and Y. Wang (2016), Seasonal and event-based drivers of runoff and phosphorus export through agricultural tile drains under sandy loam soil in a cool temperate region, *Hydrol. Process.*, *30*(15), 2644-2656.

Le, P. V., and P. Kumar (2017), Interaction between ecohydrologic dynamics and microtopographic variability under climate change, *Water Resources Research*, *53*(10), 8383-8403.

Liu, W., M. A. Youssef, F. P. Birgand, G. M. Chescheir, S. Tian, and B. M. Maxwell (2020), Processes and mechanisms controlling nitrate dynamics in an artificially drained field: Insights from high-frequency water quality measurements, *Agricultural Water Management*, *232*, 106032.

Lloyd, C., J. Freer, P. Johnes, and A. Collins (2016), Testing an improved index for analysing storm discharge-concentration hysteresis, *Hydrol. Earth Syst. Sci.*, *20*(2), 625-632.

Macrae, M., M. English, S. Schiff, and M. Stone (2007), Intra-annual variability in the contribution of tile drains to basin discharge and phosphorus export in a first-order agricultural catchment, *Agricultural Water Management*, *92*(3), 171-182.

Macrae, M., M. English, S. Schiff, and M. Stone (2010), Influence of antecedent hydrologic conditions on patterns of hydrochemical export from a first-order agricultural watershed in Southern Ontario, Canada, *J. Hydrol.*, *389*(1-2), 101-110.

Macrae, M., G. Ali, K. King, J. Plach, W. Pluer, M. Williams, M. Morison, and W. Tang (2019), Evaluating Hydrologic Response in Tile-Drained Landscapes: Implications for Phosphorus Transport, *Journal of environmental quality*, *48*(5), 1347-1355.

McDonnell, J. J., C. Spence, D. J. Karran, H. J. van Meerveld, and C. J. Harman (2021), Fill-and-Spill: A Process Description of Runoff Generation at the Scale of the Beholder, *Water Resources Research*, *57*(5).

McGuire, K. J., and J. J. McDonnell (2010), Hydrological connectivity of hillslopes and streams: Characteristic time scales and nonlinearities, *Water Resources Research*, *46*(10).

McMillan, S. K., H. F. Wilson, C. L. Tague, D. M. Hanes, S. Inamdar, D. L. Karwan, T. Loecke, J. Morrison, S. F. Murphy, and P. Vidon (2018), Before the storm: antecedent conditions as regulators of hydrologic and biogeochemical response to extreme climate events, *Biogeochemistry*, 1-15.

NRCS (2020), Web Soil Survey. Natural Resources Conservation Service, United States Department of Agriculture: http://websoilsurvey.sc.egov.usda.gov/. Date accessed: June 2020.

Outram, F. N., R. J. Cooper, G. Sünnenberg, K. M. Hiscock, and A. A. Lovett (2016), Antecedent conditions, hydrological connectivity and anthropogenic inputs: Factors affecting nitrate and phosphorus transfers to agricultural headwater streams, *Science of the Total Environment*, *545*, 184-199.

Penna, D., H. Tromp-van Meerveld, A. Gobbi, M. Borga, and G. Dalla Fontana (2011), The influence of soil moisture on threshold runoff generation processes in an alpine headwater catchment, *Hydrol. Earth Syst. Sci.*, *15*(3), 689-702.

Power, J., and J. Schepers (1989), Nitrate contamination of groundwater in North America, *Agriculture, ecosystems & environment*, *26*(3-4), 165-187.

Randall, G. W., and D. J. Mulla (2001), Nitrate nitrogen in surface waters as influenced by climatic conditions and agricultural practices, *Journal of Environmental Quality*, *30*(2), 337-344.

Rhoads, B. L., Q. W. Lewis, and W. Andresen (2016), Historical changes in channel network extent and channel planform in an intensively managed landscape: Natural versus human-induced effects, *Geomorphology*, *252*, 17-31.

Rodvang, S., and W. Simpkins (2001), Agricultural contaminants in Quaternary aquitards: A review of occurrence and fate in North America, *Hydrogeology Journal*, *9*(1), 44-59.

Rose, L. A., D. L. Karwan, and S. E. Godsey (2018), Concentration–discharge relationships describe solute and sediment mobilization, reaction, and transport at event and longer timescales, *Hydrol. Process.*, *32*(18), 2829-2844.

Royer, T. V., M. B. David, and L. E. Gentry (2006), Timing of Riverine Export of Nitrate and Phosphorus from Agricultural Watersheds in Illinois: Implications for Reducing Nutrient Loading to the Mississippi River, *Environmental Science & Technology*, *40*(13), 4126-4131.

Saadat, S., L. Bowling, J. Frankenberger, and E. Kladivko (2018), Nitrate and phosphorus transport through subsurface drains under free and controlled drainage, *Water Research*, *142*, 196-207.

Sacks, W. J., and C. J. Kucharik (2011), Crop management and phenology trends in the US Corn Belt: Impacts on yields, evapotranspiration and energy balance, *Agricultural and Forest Meteorology*, *151*(7), 882-894.

Scaife, C. I., and L. E. Band (2017), Nonstationarity in threshold response of stormflow in southern Appalachian headwater catchments, *Water Resources Research*, *53*(8), 6579-6596.

Schilling, K., and Y. Zhang (2004), Baseflow contribution to nitrate-nitrogen export from a large, agricultural watershed, USA, *J. Hydrol.*, *295*(1), 305-316.

Schilling, K., and M. Helmers (2008), Effects of subsurface drainage tiles on streamflow in Iowa agricultural watersheds: Exploratory hydrograph analysis, *Hydrological Processes: An International Journal*, *22*(23), 4497-4506.

Shaw, R. H. (1963), Estimation of soil moisture under corn, *Iowa Agriculture and Home Economics Experiment Station Research Bulletin*, *34*(520), 1.

Sims, J. T., R. R. Simard, and B. C. Joern (1998), Phosphorus loss in agricultural drainage: Historical perspective and current research, *Journal of environmental quality*, *27*(2), 277-293.

Soulsby, C., C. Birkel, J. Geris, J. Dick, C. Tunaley, and D. Tetzlaff (2015), Stream water age distributions controlled by storage dynamics and nonlinear hydrologic connectivity: Modeling with high-resolution isotope data, *Water resources research*, *51*(9), 7759-7776.

Spence, C. (2007), On the relation between dynamic storage and runoff: A discussion on thresholds, efficiency, and function, *Water Resources Research*, *43*(12).

Stieglitz, M., J. Shaman, J. McNamara, V. Engel, J. Shanley, and G. W. Kling (2003), An approach to understanding hydrologic connectivity on the hillslope and the implications for nutrient transport, *Global Biogeochemical Cycles*, *17*(4).

Troch, P. A., T. Lahmers, A. Meira, R. Mukherjee, J. W. Pedersen, T. Roy, and R. Valdés-Pineda (2015), Catchment coevolution: A useful framework for improving predictions of hydrological change?, *Water Resources Research*, *51*(7), 4903-4922.

Tromp-van Meerveld, H., and J. McDonnell (2006a), Threshold relations in subsurface stormflow: 1. A 147-storm analysis of the Panola hillslope, *Water Resources Research*, *42*(2).

Tromp-van Meerveld, H., and J. McDonnell (2006b), Threshold relations in subsurface stormflow: 2. The fill and spill hypothesis, *Water Resources Research*, *42*(2).

USDA (2017), U.S. Department of Agriculture, 2017 Census of Agriculture: United States Summary and State Data, *1, Geographic Area Studies, Part 51*.

Van Meter, K. J., N. B. Basu, J. J. Veenstra, and C. L. Burras (2016), The nitrogen legacy: emerging evidence of nitrogen accumulation in anthropogenic landscapes, *Environmental Research Letters*, *11*(3), 035014.

Vaughan, M. C., W. B. Bowden, J. B. Shanley, A. Vermilyea, R. Sleeper, A. J. Gold, S. M. Pradhanang, S. P. Inamdar, D. F. Levia, and A. S. Andres (2017), High-frequency dissolved organic carbon and nitrate measurements reveal differences in storm hysteresis and loading in relation to land cover and seasonality, *Water Resources Research*, *53*(7), 5345-5363.

Vidon, P., and P. Cuadra (2010), Impact of precipitation characteristics on soil hydrology in tile-drained landscapes, *Hydrol. Process.*, *24*(13), 1821-1833.

Weiler, M., J. J. McDonnell, I. Tromp-van Meerveld, and T. Uchida (2005), Subsurface stormflow, *Encyclopedia of hydrological sciences*.

Williams, M., K. King, and N. Fausey (2015), Contribution of tile drains to basin discharge and nitrogen export in a headwater agricultural watershed, *Agricultural water management*, *158*, 42-50.

Williams, M., S. Livingston, C. Penn, D. Smith, K. King, and C.-h. Huang (2018), Controls of event-based nutrient transport within nested headwater agricultural watersheds of the western Lake Erie basin, *J. Hydrol.*, *559*, 749-761.

Wilson, C. G., et al. (2018), The Intensively Managed Landscape Critical Zone Observatory: A Scientific Testbed for Understanding Critical Zone Processes in Agroecosystems, *Vadose Zone J.*, *17*(1), 180088.

Woo, D. K., and P. Kumar (2016), Mean age distribution of inorganic soil-nitrogen, *Water Resources Research*, *52*(7), 5516-5536.

Woo, D. K., and P. Kumar (2017), Role of micro-topographic variability on the distribution of inorganic soil-nitrogen age in intensively managed landscape, *Water Resources Research*, *53*(10), 8404-8422.

Woo, D. K., and P. Kumar (2019), Impacts of Subsurface Tile Drainage on Age—Concentration Dynamics of Inorganic Nitrogen in Soil, *Water Resources Research*, *55*(2), 1470-1489.

Woo, D. K., J. C. Quijano, P. Kumar, S. Chaoka, and C. J. Bernacchi (2014), Threshold Dynamics in Soil Carbon Storage for Bioenergy Crops, *Environmental Science & Technology*, *48*(20), 12090-12098.

Zulauf, C., and B. Brown (2019), Use of Tile, 2017 US Census of Agriculture, *farmdoc daily*, *9*(141), Department of Agricultural and Consumer Economics, University of Illinois at Urbana-Champaign.